Supporting information for:

Critical Sequence Hot-spots for Binding of nCOV-2019 to ACE2 as Evaluated by Molecular Simulations

Mahdi Ghorbani[1,3], Bernard Brooks[3], Jeffery Klauda[1,2]
[1]Department of Chemical and Biomolecular Engineering, [2]Biophysics Graduate Program, University of Maryland, College Park, MD 20742, USA
[3]Laboratory of Computational Biology, National, Heart, Lung and Blood Institute, National Institutes of Health, Bethesda, Maryland 20824, USA
*Corresponding Author: jbklauda@umd.edu

Table S1. Residues investigated here and their corresponding location in RBD of nCOV-2019.

residue	Location
K417	α_3
N439	α_4
G446	L_1
G447	L_1
Y449	L_1
Y453	β_5
L455	β_5
F456	L_2
Y473	β_6
A475	β_6
G476	L_3
T478	L_3
V483	L_3
E484	L_3
F486	L_3
N487	L_3
Y489	β_6
Q493	β_5
S494	β_5
G496	L_4
Q498	L_4
T500	L_4
N501	L_4
G502	L_4
Y505	α_5

Table S2. Binding free energy decomposition in $\frac{kcal}{mol}$ for 2019-nCOV, SARS-COV and mutants.

	vdw	Electro	Polar solv	SASA	total
SARS-COV	-70.07 ± 1.22	-600.14 ± 7.65	659.61 ± 8.98	-8.39 ± 0.15	-18.79 ± 1.53
SARS-D480A	-88.30 ± 0.69	-897.14 ± 3.8	972.07 ± 3.90	-10.14 ± 0.07	-23.46 ± 3.07
nCOV-2019	-89.93 ± 0.46	-746.59 ± 2.66	797.3 ± 3.12	-10.58 ± 0.05	-50.22 ± 1.93
K417A	-88.23 ± 0.58	-415.67 ± 5.07	484.87 ± 4.89	-10.29 ± 0.09	-29.56 ± 2.95
N439K	-95.4 ± 0.63	-989.84 ± 5.57	1047.70 ± 5.08	-10.86 ± 0.06	-48.27 ± 3.07
G446A	-91.9 ± 0.5	-730.12 ± 3.68	774.7 ± 4.18	-10.6 ± 0.08	-57.79 ± 2.92
G447A	-93.95 ± 0.75	-756.61 ± 4.63	803.48 ± 5.02	-11.08 ± 0.09	-58.37± 2.32
Y449A	-97.98 ± 0.56	-717.67 ± 2.71	774.49 ± 3.50	-10.80 ± 0.05	-51.91 ± 2.33
Y453A	-92.3 ± 0.65	-712.76 ± 3.61	765.63 ± 3.98	-10.96 ± 0.07	-49.98 ± 2.92
L455A	-84.96 ± 0.56	-734.72 ± 4.44	795.41 ± 4.06	-10.63 ± 0.08	-33.47 ± 2.93
F456A	-95.43 ± 0.57	-770.12 ± 3.38	832.56 ± 4.14	-11.59 ± 0.07	-44.84 ± 3.38
Y473A	-90.48 ± 0.54	-725.17 ± 4.27	779.23 ± 4.16	-10.61 ± 0.06	-47.23 ± 2.59
A475V	-93.12 ± 0.49	-712.12 ± 4.59	769.23 ± 4.71	-10.68 ± 0.08	-46.07 ± 4.11
G476A	-92.84 ± 0.57	-746.46 ± 4.92	796.97 ± 4.84	-10.99 ± 0.08	-53.57 ± 2.58
G476S	-92.25 ± 0.64	-712.08 ± 4.10	767.40 ± 4.32	-10.77 ± 0.08	-47.38 ± 2.86
T478I	-88.95 ± 0.69	-753.93 ± 4.00	797.03 ± 4.01	-10.33 ± 0.08	-56.06 ± 2.83
V483A	-90.74 ± 0.60	-737.48 ± 3.94	789.22 ± 3.74	-10.76 ± 0.07	-49.55 ± 3.17
V483F	-87.23 ± 0.6	-738.08 ± 4.73	782.82 ± 4.04	-10.59 ± 0.09	-53.70 ± 3.35
E484A	-95.7 ± 0.62	-941.2 ± 3.95	1002.21 ± 4.92	-11.15 ± 0.08	-46.67 ± 2.89
F486A	-90.07 ± 0.66	-724.64 ± 4.39	779.73 ± 5.01	-10.68 ± 0.09	-45.23 ± 3.66
N487A	-102.23 ± 0.72	-724.44 ± 3.69	791.41 ± 4.3	-11.37 ± 0.08	-46.33 ± 2.73
Y489A	-103.85 ± 0.66	-773.72 ± 3.15	827.52 ± 4.36	-11.59 ± 0.05	-61.78 ± 2.59
Q493A	-84.68 ± 0.68	-713.28 ± 3.67	758.56 ± 3.63	-9.87 ± 0.07	-48.19 ± 2.64
S494A	-94.98 ± 0.66	-736.93 ± 4.05	793.94 ± 3.84	-11.02 ± 0.07	-49.09 ± 3.26
S494P	-89.39 ± 0.60	-737.54 ± 5.25	789.35 ± 5.74	-10.67 ± 0.08	-47.90 ± 2.59
G496A	-93.17 ± 0.55	-728.93 ± 4.39	784.81 ± 4.93	-10.89 ± 0.07	-48.38 ± 2.67
Q498A	-90.48 ± 0.61	-756.18 ± 4.6	812.84 ± 4.75	-11.02 ± 0.09	-45.4 ± 2.74
T500A	-93.64 ± 0.62	-704.44 ± 4.1	769.65 ± 4.73	-10.86 ± 0.08	-39.27 ± 3.18
N501A	-88.59 ± 0.66	-730.53 ± 3.63	788.41 ± 4.3	-10.75 ± 0.08	-40.36 ± 3.3
G502A	-87.61 ± 0.63	-706.13 ± 4.56	780.08 ± 4.61	-10.51 ± 0.07	-24.31 ± 2.98
Y505A	-91.35 ± 0.7	-746.12 ± 4.31	802.16 ± 5.29	-10.78 ± 0.08	-46.49 ± 2.92

Table S3. Details of H-bonds for mutants of nCOV-2019.

mutant	#	RBD	ACE2	Occupancy %
K417A	1	GLY502	LYS353	87
	2	ASN487	TYR83	82
	3	GLN493	GLU35	77
	4	THR500	ASP355	73
	5	TYR449	ASP38	53
N439K	1	GLY502	LYS353	85
	2	GLN493	GLU35	82
	3	ASN487	TYR83	67
	4	GLN498	ASP38	66
	5	THR500	ASP355	60
	6	LYS417	ASP30	51
	7	GLN498	LYS353	42
G446A	1	TYR449	ASP38	94
	2	GLY502	LYS353	90
	3	GLN498	ASP38	88
	4	TYR83	ASN487	79
	5	GLN493	GLU35	76
	6	THR500	ASP355	54
	7	LYS353	GLN498	51
	8	LYS353	GLY496	46
	9	TYR505	GLU37	43
G447A	1	TYR449	ASP38	92
	2	GLY502	LYS353	81
	3	GLN493	GLU35	68
	4	TYR505	GLU37	57
	5	TYR83	ASN487	53
	6	THR500	ASP355	46
	7	LYS353	GLN498	42
Y449A	1	GLY502	LYS353	78
	2	GLN493	GLU35	72
	3	THR500	ASP355	69
	4	LYS417	ASP30	66
	5	GLN493	LYS31	56
	6	TYR489	TYR83	47
	7	GLY496	LYS353	41
	8	Gly485	TYR83	40
Y453A	1	GLY502	LYS353	84
	2	ASN487	TYR83	78
	3	GLN493	GLU35	77
	4	TYR505	GLU37	67
	5	THR500	ASP355	56
	6	TYR449	ASP38	41
L455A	1	TYR449	ASP38	93
	2	GLY502	LYS353	88
	3	ASN487	TYR83	77
	4	LYS417	ASP30	71
	5	TYR505	GLU37	60
	6	GLN493	GLU35	58
	7	GLN498	LYS353	55
	8	GLY496	LYS353	40
F456A	1	GLY502	LYS353	83
	2	ASN487	TYR83	79
	3	GLN498	LYS353	75
	4	LYS417	ASP30	74
	5	TYR505	GLU37	70
	6	THR500	ASP355	69
	7	GLN493	GLU35	63
Y473A	1	GLY502	LYS353	88
	2	ASN487	TYR83	82
	3	GLN493	GLU35	77
	4	GLN498	ASP38	69
	5	THR500	ASP355	51
	6	GLN498	LYS353	46
	7	TYR505	GLU37	41
A475V	1	GLY502	LYS353	84
	2	GLN493	GLU35	83
	3	GLN498	ASP38	70
	4	ASN487	TYR83	68
	5	THR500	ASP355	64
	6	GLN498	LYS353	42
G476A	1	GLY502	LYS353	85
	2	TYR449	ASP38	78
	3	GLN493	GLU35	77
	4	TYR505	ALA386	75
	5	GLN498	ASP38	73
	6	TYR83	ASN487	70
	7	LYS353	GLN498	41
G476S	1	GLN493	GLU35	88
	2	TYR449	ASP38	84
	3	GLY502	LYS353	83
	4	ASN487	TYR83	69
	5	THR500	TYR41	55
	6	TYR505	GLU37	52
	7	GLN498	ASP38	52
	8	GLY496	LYS353	49
	9	GLN498	LYS353	46

Table S3. (continued)

mutant	#	RBD	ACE2	Occupancy %
T478I	1	TYR449	ASP38	95
	2	GLY502	LYS353	88
	3	GLN498	ASP38	82
	4	GLN493	GLU35	78
	5	ASN487	TYR83	70
	6	TYR505	GLU37	59
	7	Gly496	LYS353	40
	8	GLN498	LYS353	47
	9	THR500	ASP355	43
V483A	1	TYR449	ASP38	94
	2	GLY502	LYS353	89
	3	GLN498	ASP38	88
	4	GLN493	GLU35	79
	5	ASN487	TYR83	74
	6	LYS417	ASP30	57
	7	GLN498	LYS353	53
	8	TYR505	GLU37	44
	9	THR500	TYR41	44
V483F	1	TYR449	ASP38	92
	2	GLY502	LYS353	84
	3	ASN487	TYR83	74
	4	LYS417	ASP30	65
	5	GLN498	ASP38	58
	6	TYR505	GLU37	53
	7	GLY496	LYS353	51
	8	THR500	TYR41	44
	9	GLN498	LYS353	42
E484A	1	GLY502	LYS353	85
	2	GLN493	GLU35	83
	3	TYR83	ASN487	72
	4	TYR505	GLU37	68
	5	LYS417	ASP30	47
	6	THR500	ASP355	46
F486A	1	GLY502	LYS353	82
	2	GLN493	GLU35	78
	3	ASN487	TYR83	78
	4	THR500	ASP355	74
	5	TYR449	ASP38	60
	6	TYR505	ALA386	56
	7	LYS417	ASP30	44
	8	GLY496	LYS353	41

mutant	#	RBD	ACE2	Occupancy %
N487A	1	THR500	ASP355	87
	2	GLY502	LYS353	81
	3	ARG403	GLU37	73
	4	GLN498	LYS353	62
	5	GLN493	GLU35	61
	6	GLU484	LYS31	45
Y489A	1	TYR449	ASP38	89
	2	GLY502	LYS353	87
	3	GLN493	GLU35	82
	4	THR500	ASP355	65
	5	GLN498	ASP38	80
	6	LYS417	ASP30	54
	7	TYR505	GLU37	54
	8	ASN487	TYR83	43
	9	GLN498	LYS353	40
	10	GLN493	LYS31	67
	11	GLY496	LYS353	42
Q493A	1	TYR449	ASP38	95
	2	GLY502	LYS353	87
	3	GLN498	ASP38	80
	4	ASN487	TYR83	78
	5	TYR505	GLU37	61
	6	GLN498	LYS353	50
	7	LYS417	ASP30	49
	8	THR500	TYR41	47
	9	GLY496	LYS353	43
S494A	1	GLY502	LYS353	88
	2	GLN498	ASP38	87
	3	TYR83	ASN487	82
	4	GLN493	GLU35	73
	5	TYR505	GLU37	67
	6	THR500	ASP355	65
	7	LYS417	ASP30	65
S494P	1	GLN493	GLU35	91
	2	TYR449	ASP38	85
	3	GLY502	LYS353	85
	4	ASN487	TYR83	72
	5	THR500	TYR41	47
	6	TYR505	GLU37	50
	7	GLN498	ASP38	52
	8	GLY496	LYS353	43
	9	GLN498	LYS353	48

Table S3. (continued)

mutant	#	RBD	ACE2	Occupancy %
G496A	1	GLY502	LYS353	86
	2	GLN493	GLU35	80
	3	TYR83	ASN487	72
	4	THR500	ASP355	59
	5	TYR449	ASP38	55
	6	GLN498	ASP38	44
Q498A	1	TYR449	ASP38	86
	2	GLY502	LYS353	84
	3	ASN487	TYR83	78
	4	GLN493	GLU35	68
	5	LYS417	ASP30	62
	6	THR500	ASP355	58
	7	TYR453	HIS34	55
	8	TYR505	GLU37	48
T500A	1	GLY502	LYS353	82
	2	GLN493	GLU35	75
	3	TYR83	ASN487	74
	4	LYS353	GLY496	70
	5	GLN42	GLN498	66
	6	LYS353	GLN498	61
	7	LYS417	ASP30	53
	8	GLN498	GLN42	48
	9	TYR505	GLU37	47
N501A	1	TYR449	ASP38	84
	2	GLY502	LYS353	80
	3	GLN498	ASP38	79
	4	ASN487	TYR83	77
	5	GLN493	GLU35	73
	6	TYR505	GLU37	63
	7	LYS417	ASP30	61
	8	THR500	ASP355	52
	9	GLN498	LYS353	44
G502A	1	ASN487	TYR83	77
	2	GLN493	GLU35	77
	3	LYS417	ASP30	61
	4	TYR505	GLU37	47
Y505A	1	GLY502	LYS353	88
	2	ASN487	TYR83	82
	3	GLN493	GLU35	78
	4	GLN498	ASP38	78
	5	GLN498	LYS353	68
	6	THR500	ASP355	67
	7	GLN493	LYS31	50

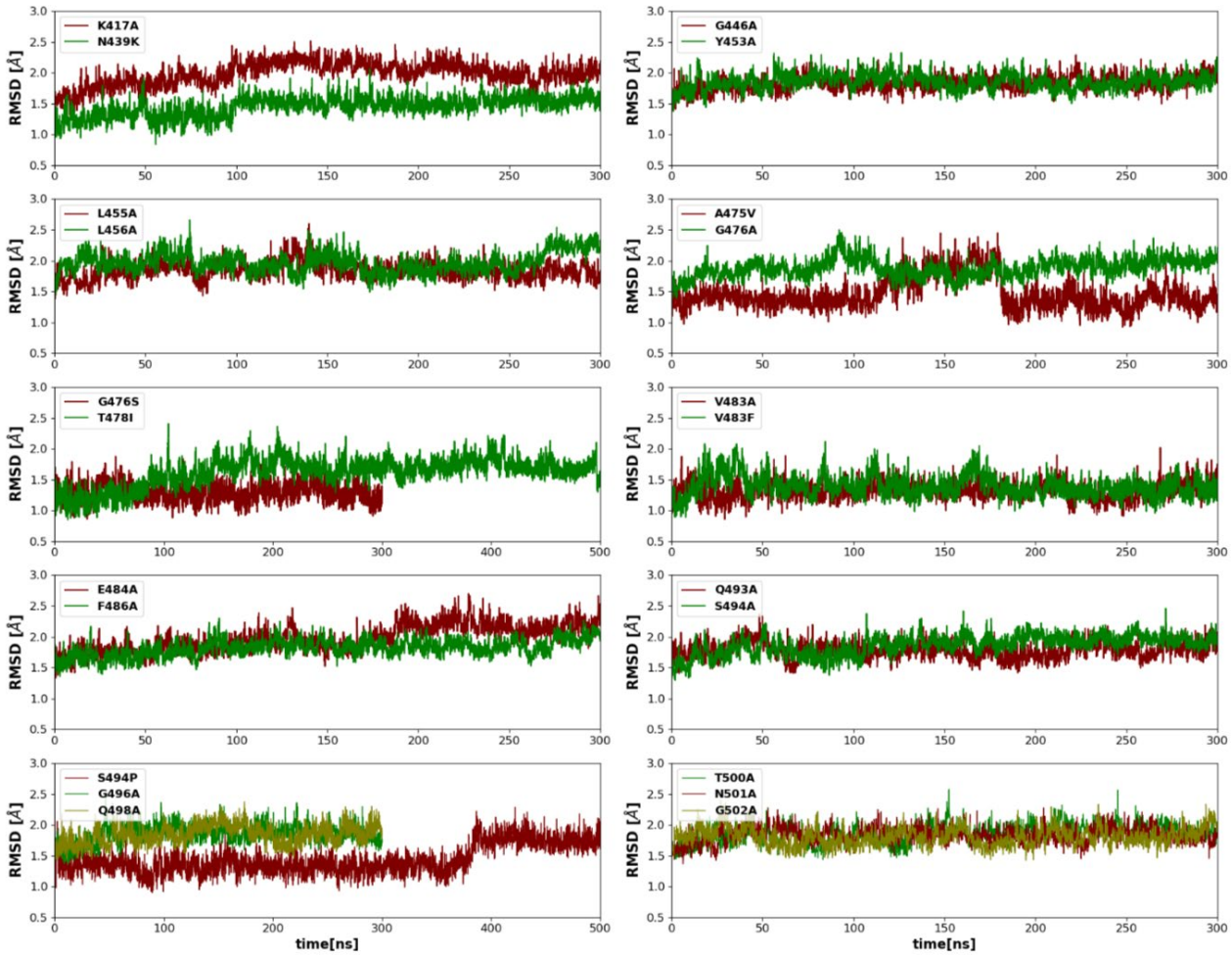

Figure S1. RMSD plots for mutations in nCOV-2019.

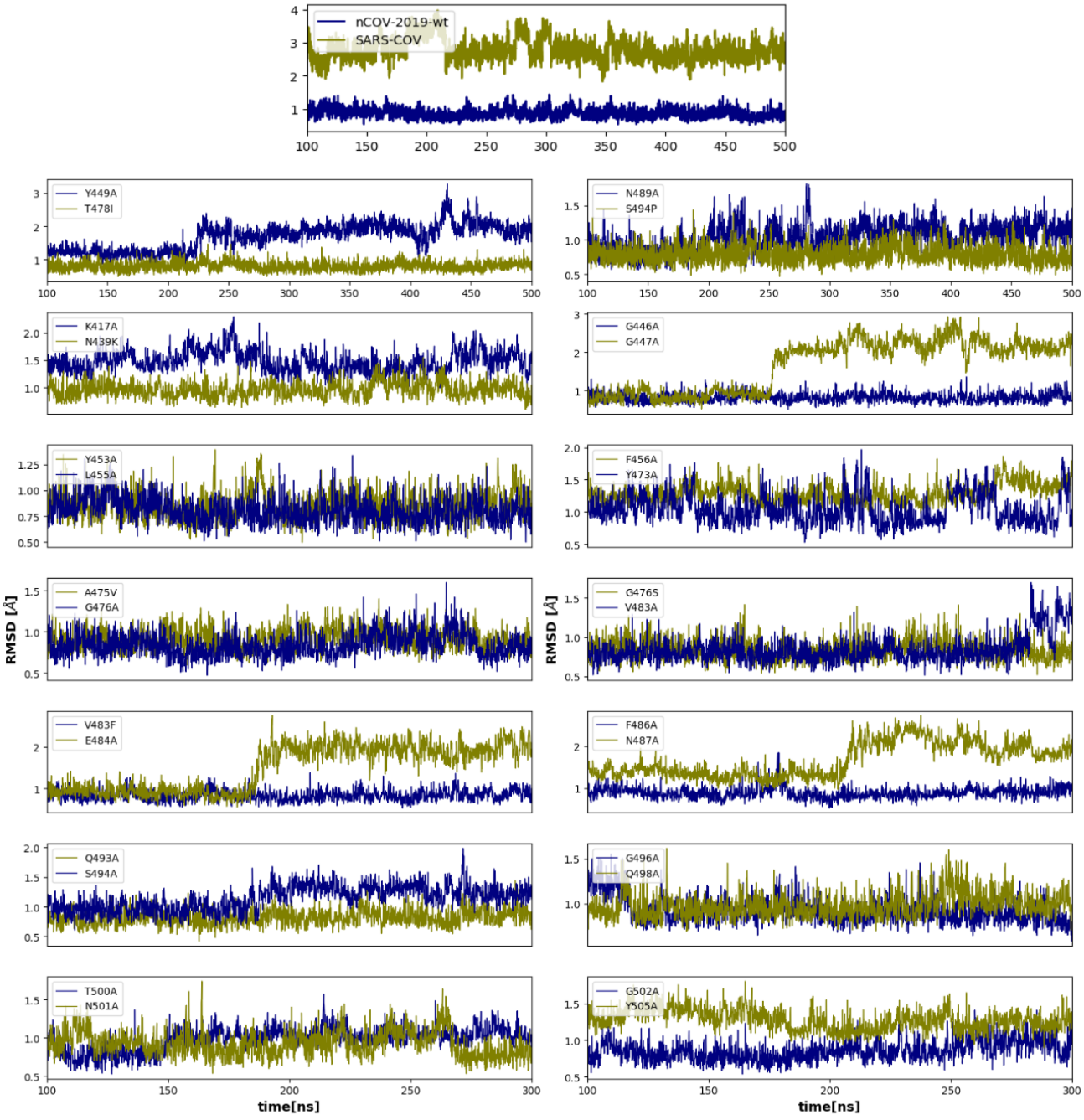

Figure S2. Loop RMSD for nCOV-2019, SARS-COV and all mutant systems.

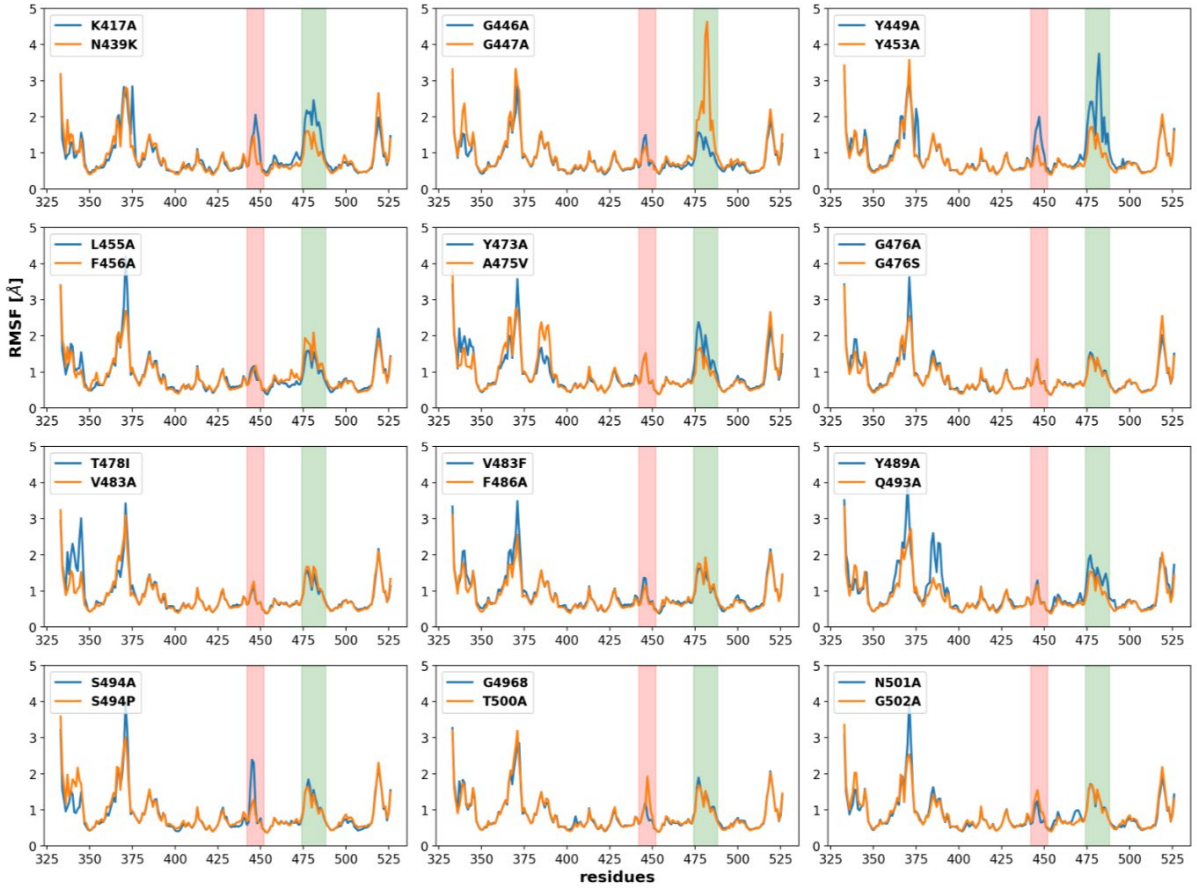

Figure S3. RMSF plots for mutations of nCOV-2019.

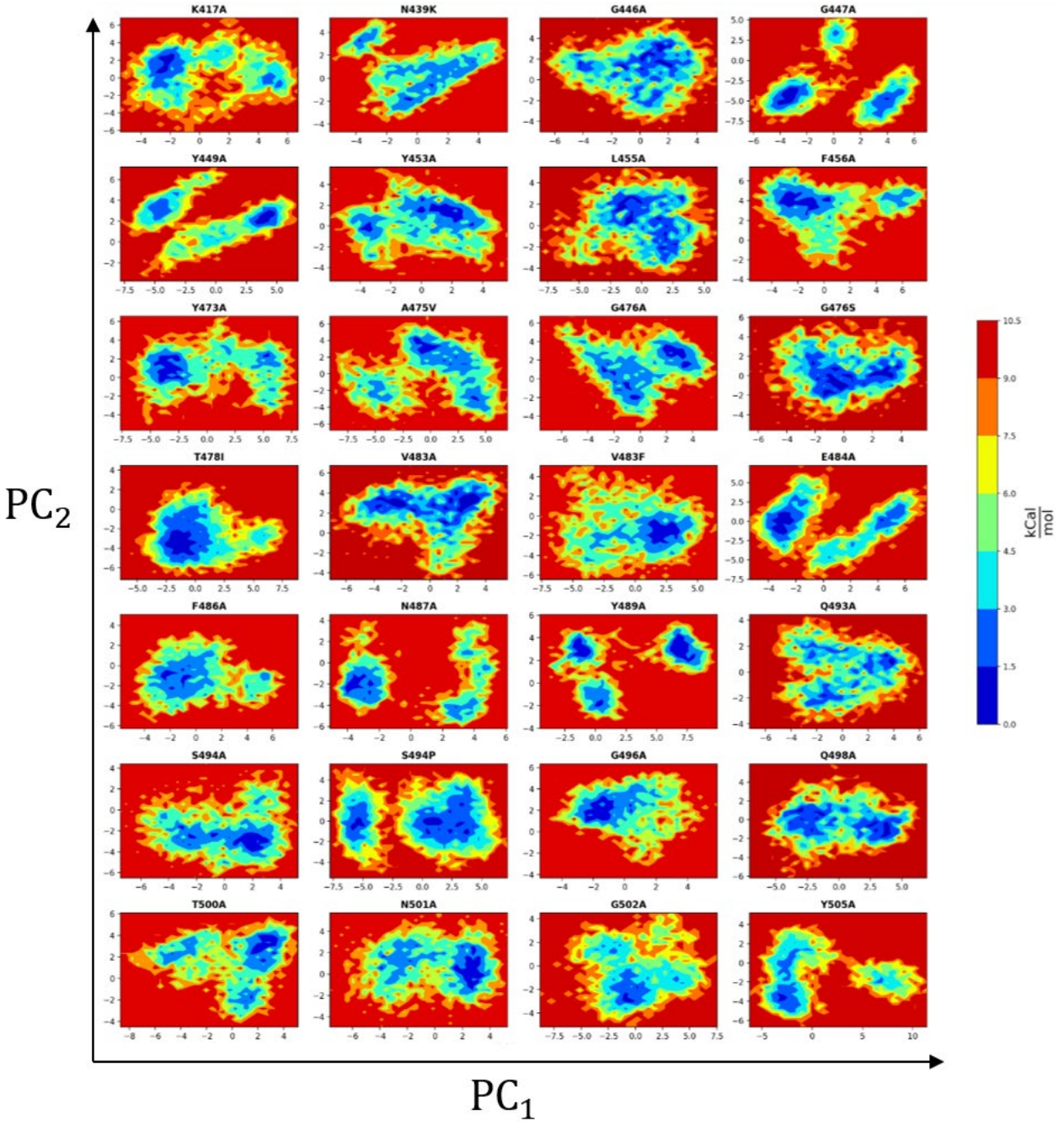

Figure S4. Free energy landscapes for mutants of nCOV-2019.

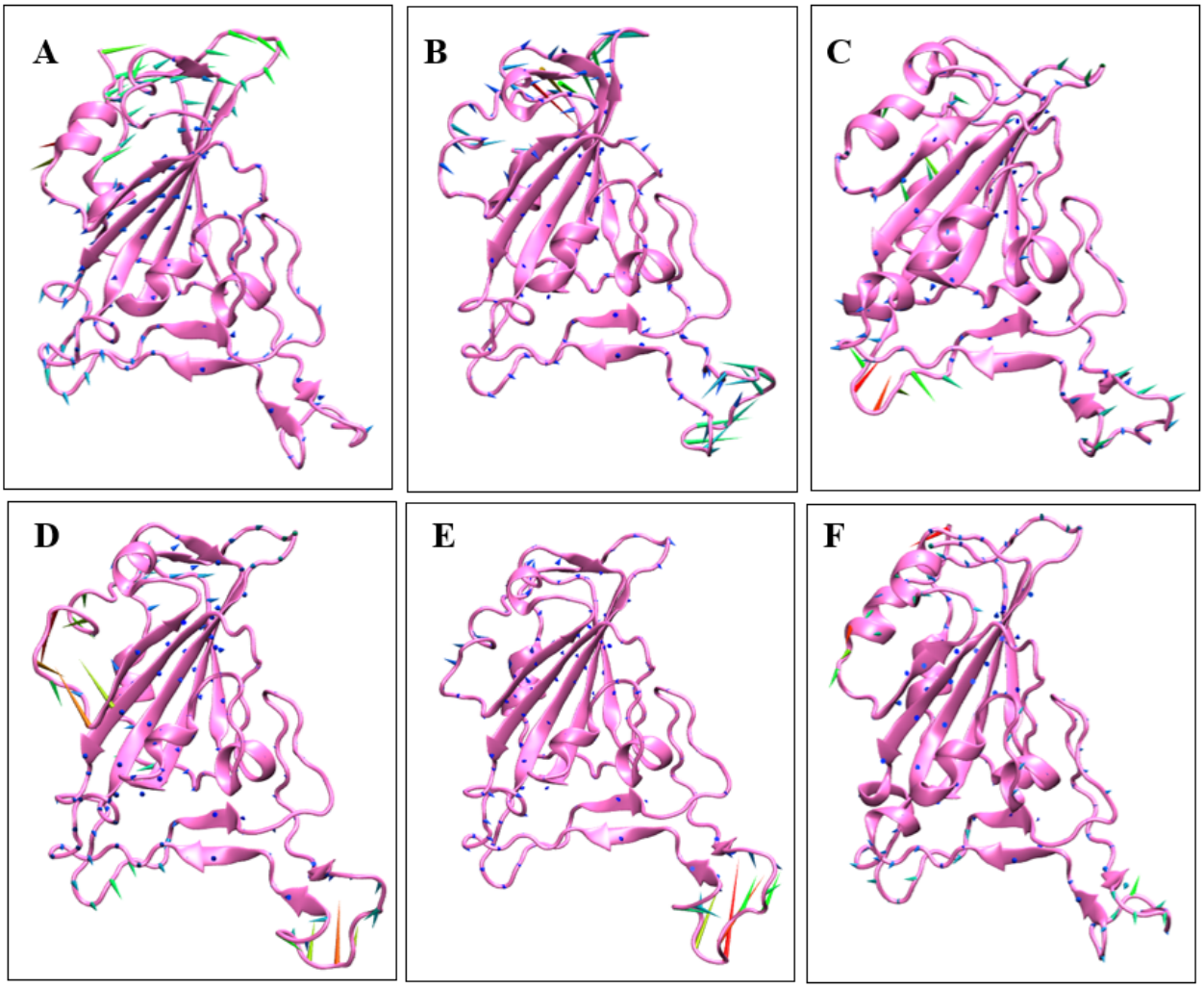

Figure S5. Porcupine plots for A) nCOV-2019 B) SARS-COV C) N487A D) Y449A E) G447A F) 18-Glu484. Arrows show the direction of movement for the C_α atoms and length of arrows show the magnitude of the motion. longer arrows are red and shorter arrows are blue.

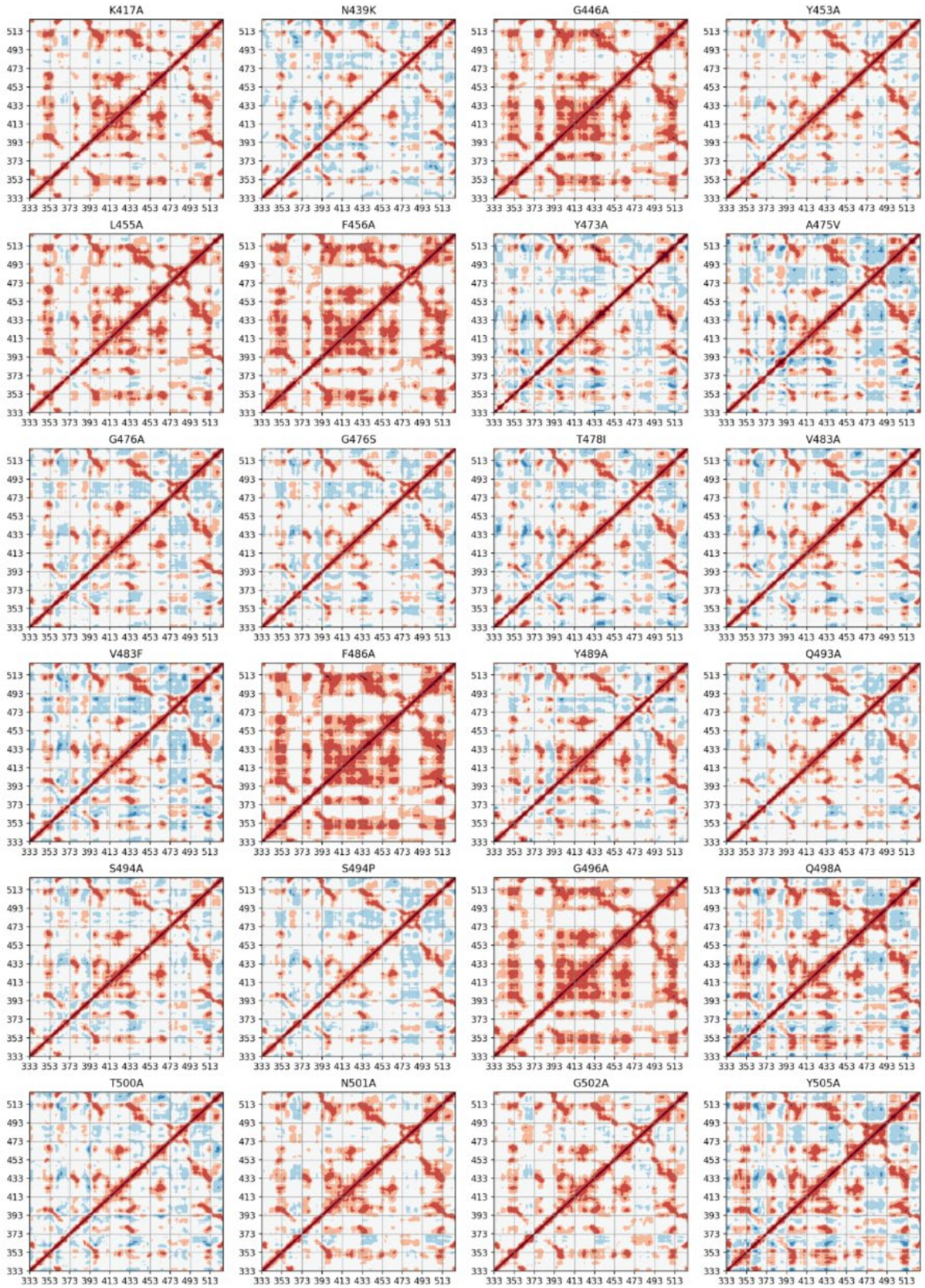

Figure S6. DCCM for mutants of nCOV-2019.

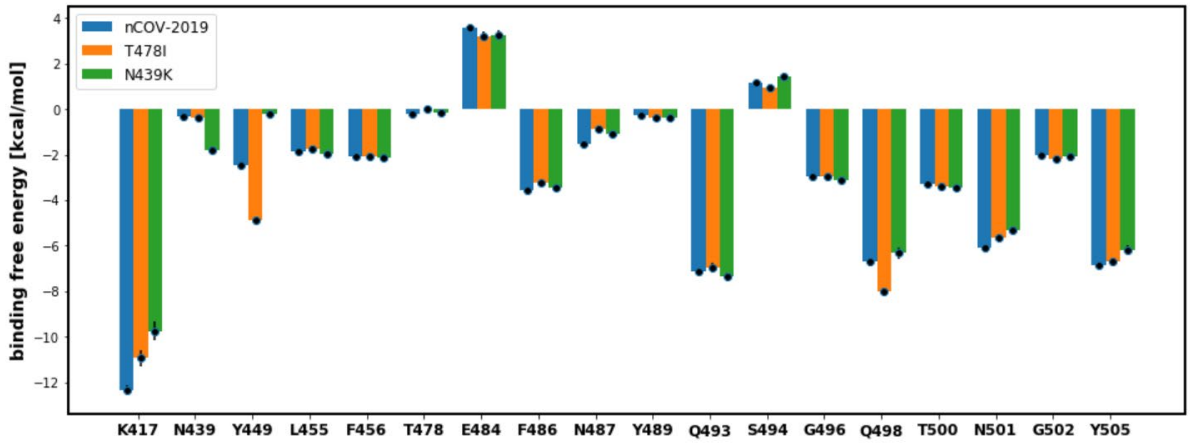

Figure S7. Binding energy decomposition for systems: nCOV-2019, T478I and N439K.